Subband structures of GaAs/$Al_xGa_{1-x}As$ multiple quantum wells

Y. Fu and K. A. Chao*
Department of Physics and Measurement Technology, University of Linköping, S-581 83 Linköping, Sweden
(Received 22 March 1989)

We solve the one-dimensional Schrödinger equation with a periodic potential and a kinetic-energy operator $-\frac{1}{2}m^{\alpha}[\hbar(d/dz)]m^{\beta}[\hbar(d/dz)]m^{\alpha}$, where $2\alpha+\beta=-1$ and the mass **m** depends on z. With the effective-mass theory, we have derived the subband structures of several GaAs/$Al_xGa_{1-x}As$ multiple-quantum-well samples. When we fit our calculated intersubband transition energies to optical data by adjusting the β and the conduction-band offset coefficient Q, the fit is not sensitive to β, which can be explained from our analytical formula. However, the results depend on the value of Q. We obtain best fits around $0.82 \le Q \le 0.89$ without exciton correction. With the exciton binding energy properly deduced, good fits are also obtained when we set $Q \approx 0.65$.

I. INTRODUCTION

The quantum nature of semiconductor heterostructures, quantum wells, and superlattices have received considerable attention recently. Besides their technological importance in high-speed electronics, the model system of these materials has intrinsic theoretical interest. In the x-y plane which is assumed to be parallel to the interfaces these materials have perfect translational symmetry. Therefore, a simple one-dimensional model with the effective-mass approximation has generally been used to study the quantum-mechanical states of electrons and holes in these materials. However, the abrupt change of chemical composition across each sharp interface introduces a position-dependent effective mass $m(z)$. One elementary problem is then to establish the proper form of the kinetic-energy ($[1/2m(z)]p_z^2$) operator for the effective-mass theory.

Several forms of the kinetic-energy operator were considered,[1-3] all of which have the general form[2,4]

$$\frac{1}{2}[m(z)]^{\alpha}\left[-i\hbar\frac{d}{dz}\right][m(z)]^{\beta}\left[-i\hbar\frac{d}{dz}\right][m(z)]^{\alpha}$$

with $2\alpha+\beta=-1$. When this form of operator is used in the one-dimensional Schrödinger equation, it has been shown[4] that the envelope-function $\psi(z)$ matching conditions across a sharp interface are in the continuity of $[m(z)]^{\alpha}\psi(z)$ and $[m(z)]^{\alpha+\beta}d\psi(z)/dz$. Morrow has analyzed several existing model calculations[5] within the framework of the effective-mass theory, and found that the works of White and Sham[6] and of Kahen and Leburton[7] correspond to $\beta=-1$, while the works of Zhu and Kroemer[3] and of Ando and Mori[8] correspond to $\beta=0$. Using the simple Kronig-Penney model for a GaAs/$Al_xGa_{1-x}As$ heterojunction with $0<x<0.45$, Morrow[5] has estimated $\beta\approx 0$ independent of x. Nevertheless, very recent works[9-11] reached an entirely different conclusion, $\beta\approx -1$.

One thus has to turn to experiments in order to be able to determine the correct value of β. In this respect, valuable information can be obtained through the optical-absorption, the luminescence, and the photoreflectance measurements.

In Sec. II we formulate a numerical computation scheme to solve the one-dimensional Schrödinger equation with an arbitrary periodic potential, and use this scheme in Sec. III to derive the subband structure of a GaAs/$Al_xGa_{1-x}As$ multiple-quantum-well system. When we fit our calculated transition energies to experimental data, we find in Sec. IV A that the results are not sensitive to the value of β, but rather depend on the conduction-band offset coefficient Q which is defined in Fig. 1. In Sec. IV B we further discover that in order to determine the value of Q, one must calculate not only the intersubband transition energies, but also the intensity of each transition, as well as the exciton binding energy. Remarks on this one-dimensional model study will be given in Sec. V.

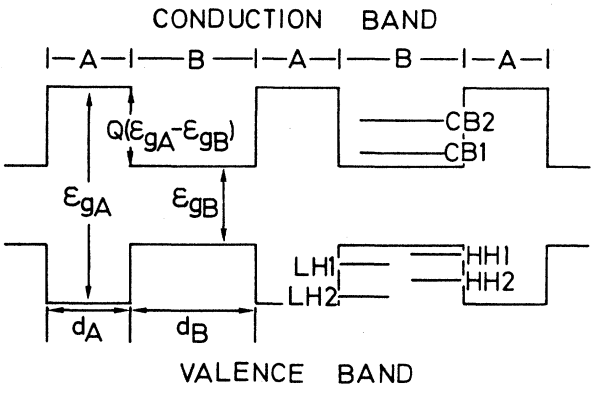

FIG. 1. A schemetic illustration of the one-dimensional model for a semiconductor MQW system and its subband positions. See text for details.

II. SUBBAND STRUCTURE

We consider a semiconductor multiple quantum well (MQW) composed of two constituent semiconductors A and B. Let the interfaces be parallel to the x-y plane, and the layer thickness of the pure A (or B) material be d_A (or d_B). In the effective-mass theory, the eigenfunction of each constituent semiconductor can be expressed as the product of an envelope function and a band state. Because the MQW to be studied in the later sections is $GaAs/Al_xGa_{1-x}As$, we can assume for each constituent semiconductor a conduction (or valence) band which has a nondegenerate minimum (or maximum) at $k=0$ with a scalar effective mass. Along the z axis which is perpendicular to the interfaces, the bottom of the conduction band and the top of the valence band are schematically illustrated in Fig. 1. Although we will calculate the subband energies both for electrons in the conduction band (CB) (such as levels CB1 and CB2) and for light (LH) and heavy (HH) holes in the valence band (such as levels LH1,LH2 and HH1,HH2), it is sufficient to present the detailed mathematical analysis for electrons only.

With such simplifications, the conduction-band envelope function $\psi(z)$ satisfies the effective-mass Schrödinger equation

$$\{-\tfrac{1}{2}\hbar^2[m(z)]^{\alpha}(d/dz)[m(z)]^{\beta}(d/dz)[m(z)]^{\alpha} + E_c(z)\}\psi(z)=E\psi(z)\ , \quad (1)$$

where $2\alpha+\beta=-1$, and $E_c(z)$ is the bottom of the conduction band specified in Fig. 1. With a constituent A or B semiconductor, (1) reduces simply to

$$[-(\hbar^2/2m_A)(d^2/dz^2)+E_{cA}-E]\psi_A(z)=0 \quad \text{for } n(d_A+d_B)<z<n(d_A+d_B)+d_A\ , \quad (2a)$$

$$[-(\hbar^2/2m_A)(d^2/dz^2)+E_{cB}-E]\psi_B(z)=0 \quad \text{for } n(d_A+d_B)-d_B<z<n(d_A+d_B)\ , \quad (2b)$$

where n is an integer, and m_A and E_{cA} (or m_B and E_{cB}) are, respectively, the effective mass and the conduction-band minimum of the constituent A (or B) semiconductor. We notice from Fig. 1 that $E_{cA}=E_{cB}+Q(E_{gA}-E_{gB})$, where Q is the conduction-band offset coefficient.

We divide the layer thickness d_A (or d_B) into $N(A)$ [or $N(B)$] equal intervals of length Δ_A (or Δ_B). For sufficiently large $N(A)$ and $N(B)$, by standard transfer matrix technique we have the recursion relations

$$\begin{bmatrix}\psi_A(d_A)\\ \psi'_A(d_A)\end{bmatrix} = \left[\prod_{n=1}^{N(A)}\begin{bmatrix}1 & \Delta_A\\ 2m_A(E_{cA}-E)\Delta_A/\hbar^2 & 1\end{bmatrix}\right]\begin{bmatrix}\psi_A(0)\\ \psi'_A(0)\end{bmatrix} \quad (3a)$$

and

$$\begin{bmatrix}\psi_B(d_A+d_B)\\ \psi'_B(d_A+d_B)\end{bmatrix} = \left[\prod_{n=1}^{N(B)}\begin{bmatrix}1 & \Delta_B\\ 2m_B(E_{cB}-E)\Delta_B/\hbar^2 & 1\end{bmatrix}\right]\begin{bmatrix}\psi_B(d_A)\\ \psi'_B(d_A)\end{bmatrix}\ . \quad (3b)$$

Using the matching conditions at the interfaces

$$\begin{bmatrix}\psi_B(d_A)\\ \psi'_B(d_A)\end{bmatrix}=\begin{bmatrix}(m_A/m_B)^{\alpha} & 0\\ 0 & (m_A+m_B)^{\alpha+\beta}\end{bmatrix}\begin{bmatrix}\psi_A(d_A)\\ \psi'_A(d_A)\end{bmatrix}$$

and

$$\begin{bmatrix}\psi_A(0)\\ \psi'_A(0)\end{bmatrix}=\begin{bmatrix}(m_B/m_A)^{\alpha} & 0\\ 0 & (m_B/m_A)^{\alpha+\beta}\end{bmatrix}\begin{bmatrix}\psi_B(0)\\ \psi'_B(0)\end{bmatrix}\ ,$$

then (3a) and (3b) are combined into

$$\begin{bmatrix}\psi_B(d_A+d_B)\\ \psi'_B(d_A+d_B)\end{bmatrix}=T(E)\begin{bmatrix}\psi_B(0)\\ \psi'_B(0)\end{bmatrix}\ , \quad (4)$$

where

$$T(E)=\left[\prod_{n=1}^{N(B)}\begin{bmatrix}1 & \Delta_B\\ 2m_B(E_{cB}-E)\Delta_B/\hbar^2 & 1\end{bmatrix}\right]\times\begin{bmatrix}1 & 0\\ 0 & (m_A/m_B)^{\beta}\end{bmatrix}\times\left[\prod_{n=1}^{N(A)}\begin{bmatrix}1 & \Delta_A\\ 2m_A(E_{cA}-E)\Delta_A/\hbar^2 & 1\end{bmatrix}\right]\times\begin{bmatrix}1 & 0\\ 0 & (m_B/m_A)^{\beta}\end{bmatrix}\ . \quad (5)$$

When we apply the periodic boundary conditions to the MQW with lattice constant $d\equiv d_A+d_B$, the Bloch theorem implies that if E is an eigenenergy of the Schrödinger equation (1), then, the eigenvalues of $T(E)$ must be $e^{\pm ikd}$ with a real value of k. The functional relation $E_\mu(k)$ gives the subband structure.

Before closing this section, it is important to mention that the above analysis is valid for a general function $E_c(z)$ in (1), even if it is random within each constituent layer, provided that the periodic boundary conditions are imposed on $E_c(z)$ with a period $d=d_A+d_B$. Therefore, if one treats $E_c(z)$ as a random potential, this computation scheme can be applied to a wide range of problems What we have studied here is the simplest case of a piecewise function $E_c(z)$.

III. CALCULATIONAL PROCEDURE

Our simple model contains many parameters; the values of which vary from material to material. Therefore, to continue our analysis we will consider a $GaAs/Al_xGa_{1-x}As$ MQW with the z axis along the [001] direction. In this case, the A constituent material is $Al_xGa_{1-x}As$, and the B constituent material is GaAs

(the same as A if $x=0$). For $x<0.4$, $Al_xGa_{1-x}As$ has a direct band gap $\varepsilon_g(x)$ at the Γ point. Around the optimum energy of each band, measured bulk material parameters of $Al_xGa_{1-x}As$ are available. The band gap varies with both the composition x and the temperature T. At room temperature $T=300$ K and for $x<0.45$, the band gap has been determined[12] as $\varepsilon_g(x)=1.425+1.155x+0.37x^2$ eV, and its temperature coefficient follows[12] $\partial\varepsilon_g(x)/\partial T=-0.395-0.115x$ meV/K. However, at low temperatures at least two formulas,[13,14] $\varepsilon_g(x)=1.512+1.455x$ eV and $\varepsilon_g(x)=1.512+1.247x$ eV, were used by different authors for $x<0.37$. Although the effective masses are insensitive to the temperature, and the effective mass of electrons in the conduction band is generally accepted[12] as $m_e^*/m_0=0.067+0.083x$, various values of the effective masses m_{hh}^* and m_{lh}^* for heavy and light holes in valence bands have been used by different authors. In our calculation, we will use two sets of hole effective masses[12,14] which are commonly used. To avoid confusion, we use the term *first set of parameter values* to represent $\varepsilon_g(x)=1.512+1.455x$ eV (for $T<100$ K), $m_{hh}^*/m_0=0.62+0.14x$, and $m_{lh}^*/m_0=0.087+0.063x$. The *second set of parameter values* refers to $\varepsilon_g(x)=1.512+1.247x$ eV (for $T<100$ K), $m_{hh}^*/m_0=0.353+0.05x$, and $m_{lh}^*/m_0=0.080+0.098x$. For both sets of parameter values, the formulas for $\varepsilon_g(x)$ at room temperature and for m_e^* are the same and as given above. It was also found experimentally[15] that for $T<150$ K the band gap is not sensitive to the temperature.

In order to make use of these bulk material parameters, we avoid considering MQW's with *thin* layer thicknesses d_A and d_B. For thicker samples, the excitonic effect is expected to be small, and so our calculation will be more realistic.

With all these specifications, there are only two free parameters left: the conduction-band offset coefficient Q and the matching-condition exponent β. They will be treated as adjustable parameters, and will be determined by fitting experimental data. The procedure is as follows. For a given MQW sample on which optical measurements were performed, we fix the values of d_A and d_B accordingly for our calculation. Next, we choose the values of Q and β and then calculate the energy subband $E_\mu(k)$ for conduction-band electrons and for valence-band heavy and light holes. The numerical solutions are derived repeatedly with decreasing values of the step lengths $\Delta_A=\Delta_B=\Delta$ until the converged subband structures $E_\mu(k)$ are reached with an accuracy of 10^{-6} meV. We can easily locate the band gaps, and to obtain the subband structures we have taken proper precautions to avoid any numerical instability. As an example, Fig. 2 shows the three lowest subbands (with indices marked as CB1, CB2, and CB3) of the conduction-band electrons in a $GaAs/Al_{0.24}Ga_{0.76}As$ MQW sample with $d_A=20$ Å and $d_B=80$ Å. In this calculation we have used the first set of parameter values, and have set $\beta=0$ and $Q=0.85$.

Knowing the subband structures, we can study the optical transitions from the valence band to the conduction band. At $k=0$, all band states have well-defined parity.

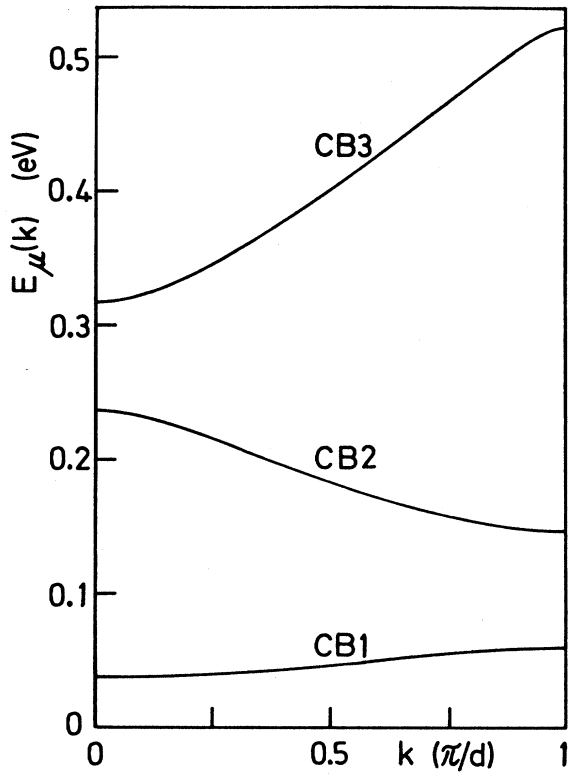

FIG. 2. Three lowest subbands of a conduction-band electron in a $GaAs/Al_{0.24}Ga_{0.76}As$ MQW sample with $d_A=20$ Å and $d_B=80$ Å, calculated with the first set of parameter values, $\beta=0$ and $Q=0.85$.

However, for finite value of k, the parity of a band state varies with k, and is no longer pure even or pure odd. Therefore, it is possible to have transition between any two subbands. If at $k=0$ a transition from the μth subband to the νth subband is allowed, the peak position of the corresponding transition intensity is at $\hbar\omega_{\nu\mu}=E_\nu(0)-E_\mu(0)$. On the other hand, if at $k=0$ the direct optical transition between the μth and the νth subbands is forbidden, the transition at certain $k_0\neq 0$ may contribute a dominating intensity to the optical-absorption spectrum around the photon energy $\hbar\bar{\omega}_{\nu\mu}=E_\nu(k_0)-E_\mu(k_0)$. For all our calculations in this paper, we will approximate $\hbar\bar{\omega}_{\nu\mu}\approx\hbar\omega_{\nu\mu}=E_\nu(0)-E_\mu(0)$. We will return to this point in the next section when we comment on the transition energies given in Table II.

We have calculated the subband structures and the associated optical spectra of many samples which have been investigated experimentally. Let us label the subbands as CB1, CB2,... for electrons with increasing energy measured from the bottom of the conduction band, and as HH1, HH2,... for heavy holes (or as LH1, LH2,... for light holes) with increasing energy measured from the top of the valence band. The relative position of these subbands are schematically shown in Fig. 1.

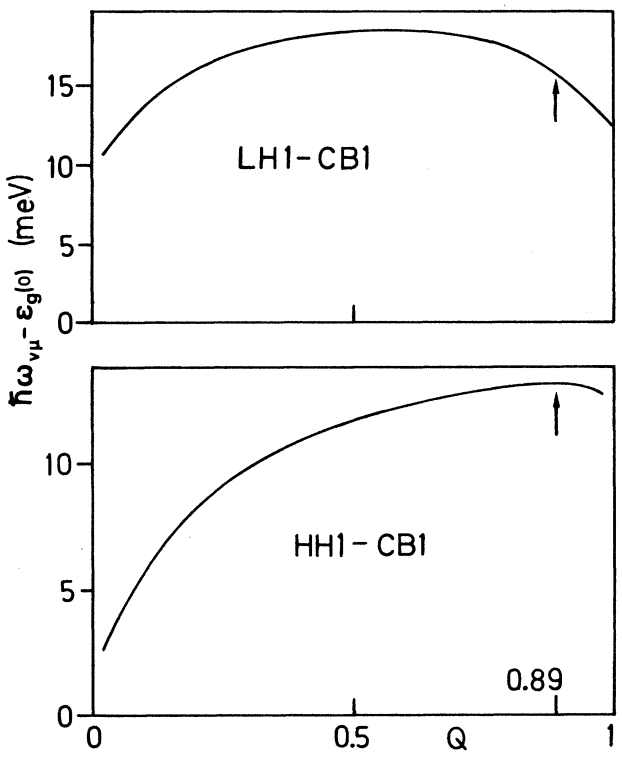

FIG. 3. Intersubband transition energies of a $GaAs/Al_{0.3}Ga_{0.7}As$ MQW sample with $d_A=19$ Å and $d_B=188$ Å, calculated with the first set of parameter values at $T=2$ K. The value of β is 0. The arrows mark the fit to the experimental values (Ref. 17).

Among all the samples we have studied, we found that the lowest optical transition energy is $\hbar\omega_{CB1,HH1}$, and the next-lowest energy is $\hbar\omega_{CB1,LH1}$. We will fit these two energies of a given sample to the two lowest-lying peaks of the corresponding measured spectrum in order to determine the values of Q and β.

We will present a specific case to illustrate our computational procedure. Consider a $GaAs/Al_{0.3}Ga_{0.7}As$ MQW sample, with the thicknesses $d_A=19$ Å for the $Al_{0.3}Ga_{0.7}As$ layers and $d_B=188$ Å for the GaAs layers. Let us for the moment use the first set of parameter values, and choose $\beta=0$ and the temperature $T=2$ K. With a given value of Q between 0 and 1, we calculate first the subband structure and then the transition energies $\hbar\omega_{CB1,HH1}$ and $\hbar\omega_{CB1,LH1}$. The excitation energies $\hbar\omega_{CB1,HH1}-\varepsilon_g(0)$ and $\hbar\omega_{CB1,LH1}-\varepsilon_g(0)$ are plotted in Fig. 3 as functions of Q. By comparing with the measured transition energies,[16] we found that at $Q=0.89$ the calculated values of both $\hbar\omega_{CB1,HH1}-\varepsilon_g(0)$ and $\hbar\omega_{CB1,LH1}-\varepsilon_g(0)$ agree well with the experimental data.

IV. RESULTS

We have used the calculational procedure described in the preceding section to analyze the subband structures of many samples with different values of x, d_A, and d_B, as well as the corresponding optical spectra which are measured at different temperatures. We have performed separate calculations using both sets of parameter values. We should particularly point out that when the experimental temperature is below 100 K, at which the gap parameter $\varepsilon_g(x)$ is insensitive to temperatures, we use both $\varepsilon_g(x)=1.512+1.455x$ eV and $\varepsilon_g=1.512+1.247x$ eV determined at $T=2$ K, while for those spectra taking around room temperature, we use the proper value of $\varepsilon_g(x)$ calculated from $\varepsilon_g(x)=1.425+1.155x+0.37x^2$ eV for $T=300$ K and its temperature coefficient.[12]

A. Determination of β and Q

In contrast to Morrow's conclusion drawn from his Kronig-Penney model calculation for a single $GaAs/Al_xGa_{1-x}As$ heterojunction, our fitting to various measured spectra (details to be given later) is insensitive to the value of β used in computations, regardless of which parameter-values set is used. With a given value of β, for any one of the samples (with various values of x, d_A, and d_B) we have studied, we can always find a value of Q in the narrow range $0.82\le Q\le 0.89$ such that the two lowest-lying peaks of the spectrum fit well to the computed energies $\hbar\omega_{CB1,LH1}$ and $\hbar\omega_{CB1,LH1}$ of the two allowed transitions from the HH1 subband to the CB1 subband and from the LH1 subband to the CB1 subband. This discovery is clearly demonstrated in Table I as an example, which is computed using the first set of parameter values at $T=2$ K for a $GaAs/Al_{0.25}Ga_{0.75}As$ MQW sample with $Q=0.85$, $d_A=25$ Å, and $d_B=150$ Å. For each transition between the μth subband and the νth subband, Table I lists two transition energies $\hbar\omega_{v\mu}$: one is calculated with $\beta=0$ and the other is calculated with $\beta=-1$. The difference between the two transition energies is too small to be resolved experimentally.

The origin of this β insensitive phenomenon is the spe-

TABLE I. Intersubband transition energies (units of MeV) of a $GaAs/Al_{0.25}Ga_{0.75}As$ MQW sample with $d_A=25$ Å and $d_B=150$ Å, calculated with the first set of parameter values at $T=2$ K. The value of Q is 0.85.

	β	CB1	CB2	CB3
LH1	0	1535.934	1586.332	1664.175
	−1	1535.854	1585.268	1665.776
LH2	0	1559.009	1609.407	1688.310
	−1	1558.448	1607.852	1687.300
LH3	0	1603.483	1653.881	1732.724
	−1	1603.744	1654.148	1732.760
HH1	0	1531.951	1582.349	1661.192
	−1	1532.317	1583.721	1661.229
HH2	0	1540.845	1591.243	1670.086
	−1	1540.844	1591.168	1669.676
HH3	0	1555.086	1605.483	1684.327
	−1	1554.610	1605.005	1683.522

cial form of β dependence of the matrix $T(E)$ given by (9). We notice that the ratio of effective-mass m_A/m_B can be expressed as $m_A/m_B=1+\alpha x$, where α is of order 1 and x is less than 0.4 for all the samples we have studied. Therefore, in the evaluation of the spectral properties of the matrix $T(E)$, there will be extensive cancellation between the contribution from the $(m_A/m_B)^\beta$ term and the contribution from the $(m_B/m_A)^\beta=(m_A/m_B)^{-\beta}$ term. On the other hand, if the sample is a single heterostructure, either $(m_B/m_A)^\beta$ or $(m_A/m_B)^\beta$ appears in a similar matrix equation, but not both. Consequently, there is no such cancellation, and so the result will have a stronger dependence on β.

We have performed another similar calculation on the same sample as the one used for Table I. Again we use the first set of parameter values as an example, but now we set $\beta=-0.5$ and calculate two transition energies for $Q=0.82$ and $Q=0.89$. The results are listed in Table II. Although the difference between the two corresponding values is still small for the two transition energies $\hbar\omega_{\mathrm{CB1,HH1}}$ and $\hbar\omega_{\mathrm{CB1,LH1}}$, for some other transitions the energy discrepancies are large enough to be detected experimentally. Therefore, the fitting of the whole spectrum is sensitive to the precise value of Q. Nevertheless, we must be aware of the following points. At $k=0$ the two transitions HH1$\Longrightarrow$CB1 and LH1$\Longrightarrow$CB1 are allowed, while some other transitions (such as LH2$\Longrightarrow$CB1) are forbidden. As we mentioned earlier, if the $\mu\Longrightarrow\nu$ subband transition is forbidden at $k=0$, we approximate the peak position $\hbar\tilde{\omega}_{\nu\mu}\approx\hbar\omega_{\mu\nu}=E_\nu(0)-E_\mu(0)$. This approximation may introduce a non-negligible error. Furthermore, with increasing subband index n, the subband structures $E_{\mathrm{CB}n}(k)$, $E_{\mathrm{LH}n}(k)$, and $E_{\mathrm{HH}n}(k)$ in Sec. II derived from a one-dimensional model become less accurate. Hence, the calculated transition energies $E_{\mathrm{CB}n}(0)-E_{\mathrm{HH}m}(0)$ and $E_{\mathrm{CB}n}(0)-E_{\mathrm{LH}m}(0)$ also become less reliable for larger n and m. Finally, the width of a measured absorption line grows with the photon energy, making the determination of the peak position increasing difficult. Taking into account these aspects, most of the high-lying transition energies are not accurately calculated theoretically and not accurately measured experimentally. Consequently, we do not expect a perfect fit between the computed and the measured spectra.

TABLE II. Intersubband transition energies (units of meV) of the same sample as for Table I, calculated with the first set of parameter values at $T=2$ K. The value of β is -0.5.

	Q	CB1	CB2	CB3
LH1	0.82	1536.794	1586.604	1664.157
	0.89	1535.004	1585.996	1665.794
LH2	0.82	1561.607	1611.417	1688.970
	0.89	1555.850	1606.842	1686.640
LH3	0.82	1606.983	1656.793	1734.346
	0.89	1599.244	1651.236	1730.038
HH1	0.82	1532.145	1581.955	1659.508
	0.89	1532.123	1583.115	1662.913
HH2	0.82	1541.505	1591.315	1668.868
	0.89	1540.104	1591.096	1670.894
HH3	0.82	1556.567	1606.367	1683.930
	0.89	1553.129	1604.121	1683.919

B. Analysis of spectra

Since the subband structure is not sensitive to the value of β (at least for the samples we have studied) regardless which set of parameters is used in our calculation, in the rest of this section we will simply set $\beta=0$. Though we found from our calculation that the power of Q lies in a narrow range $0.82\leq Q\leq 0.89$ (which agrees with the conclusion of Dingle *et al.*[17]), we are aware of the fact that the generally accepted value is $Q\approx 0.65$. Furthermore, when $Q\approx 0.65$ is used in their calculations, most authors also used the second set of parameter values. It is important to mention that the exciton effect is not considered in our analysis. The following results suggest that the neglect of exciton binding energy in our calculation may not be the reason that we have obtained a larger value of Q.

Figure 4 gives the optical-absorption coefficient[18] mea-

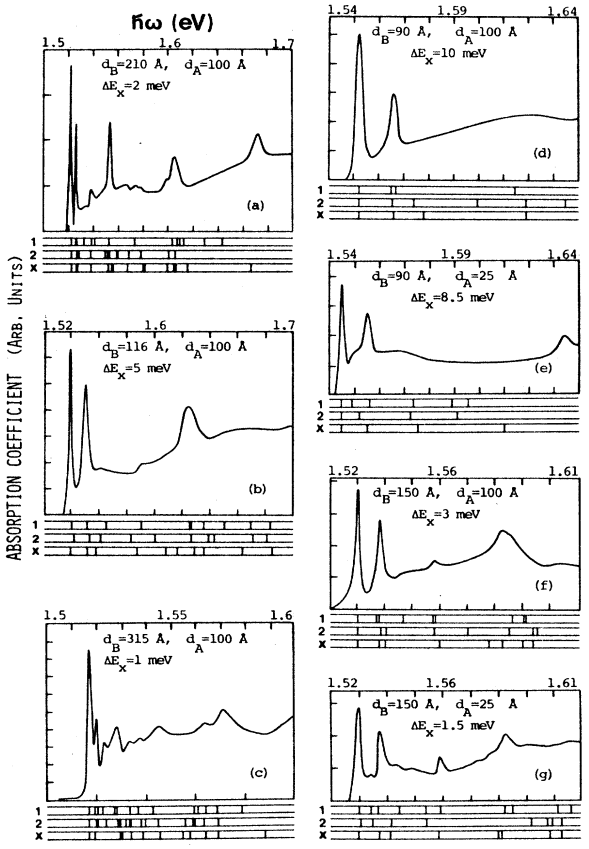

FIG. 4. A comparison between the calculated intersubband transition energies (marked by vertical bars in rows 1, 2, and X under each panel) and the measured optical-absorption spectra of various samples. See text for details.

sured at temperature $T=4.2$ K for seven GaAs/$Al_{0.25}Ga_{0.75}As$ samples of different well thickness d_B and barrier thickness d_A. The values of d_A and d_B of each sample are written in the corresponding panel. The photoluminsecence data and the photoreflectance data in Fig. 5 are measured on four samples at $T=1.8$ K [panel (a)],[16] $T=7$ K [panel (b)],[19] $T=6$ K [panel (c)],[20] and $T=300$ K [panel (d)].[21] For each sample the values of x, d_A, and d_B are specified in the panel. Under each panel, there are three rows labeled 1, 2, and X. In each row there is a sequence of vertical bars, which mark the calculated intersubband transition energies. The row 1 is calculated with the first set of parameter values and with $Q=0.89$, while the row 2 is calculated with the second set of parameter values and with $Q=0.85$. We have also performed another calculation with the second set of parameter values but with $Q=0.65$. In this last calculation, the discrepancy between the computed lowest (HH1 $\Longrightarrow$ CB1) transition energy and the observed lowest peak position is assumed to be the binding energy ΔE_X of the exciton. For every sample the value of ΔE_X is also given in the corresponding panel. After correcting each spectrum by a shift of its exciton binding energy ΔE_X, the final result is shown as row X under the panel.

The intersubband transitions for row 1, 2, and X are listed in Tables III–V, respectively. In each table the first column labels the vertical bars of a given row from the left to the right end with increasing intersubband transition energy. The other columns in each table refer to the panels in Figs. 4 and 5. For example, column 4(d) corresponds to panel (d) of Fig. 4. In our notation, $Hm \Longrightarrow n$ means the transition from the HHm subband to the CBn subband, and $Lm \Longrightarrow n$ means the transition from the LHm subband to the CBn subband. For panel (d) in Fig. 5, we have marked only the transitions with $m=n$ in order to have a clearly visible plot.

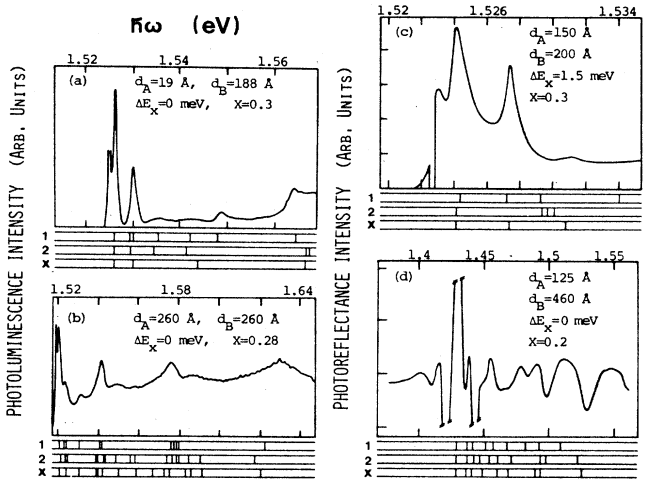

FIG. 5. A comparison between the calculated intersubband transition energies (marked by vertical bars in rows 1, 2, and X under each panel) and the measured photoluminescence and photoreflectance spectra of various samples. See text for details.

For most samples the exciton binding energy is rather small. We see in Fig. 4 the monotonic decrease of exciton binding energy with increasing well thickness, as indicated by the change of ΔE_X through the sequence of panels (d) $\Longrightarrow$ (b) $\Longrightarrow$ (f) $\Longrightarrow$ (a) $\Longrightarrow$ (c). Regardless of the value of the binding energy of the exciton, we notice that in the vicinity of almost every peak in Figs. 4 and 5, in each of the three rows 1, 2, and X, there exists at least one calculated intersubband transition energy. Therefore, without computing the intensities of all intersubband transitions,

TABLE III. Intersubband transitions corresponding to row 1 under each panel in Figs. 4 and 5. $H_m \Longrightarrow n$ (or $Lm \Longrightarrow n$) means the transition from the HHm (or LHm) subband to the CBn subband. Experimental data are from Refs. 16 and 18–21.

	Transitions for row 1 in Figs. 4 and 5										
No.	4(a)	4(b)	4(c)	4(d)	4(e)	4(f)	4(g)	5(a)	5(b)	5(c)	5(d)
1	$H1\Longrightarrow 1$	$H1\Longrightarrow 1$	$H1\Longrightarrow 1$	$H1\Longrightarrow 1$	$H1\Longrightarrow 1$	$H1\Longrightarrow 1$	$H1\Longrightarrow 1$	$H1\Longrightarrow 1$	$H1\Longrightarrow 1$	$H1\Longrightarrow 1$	$H1\Longrightarrow 1$
											$L1\Longrightarrow 1$
2	$L1\Longrightarrow 1$	$L1\Longrightarrow 1$	$L1\Longrightarrow 1$	$L1\Longrightarrow 1$	$L1\Longrightarrow 1$	$L1\Longrightarrow 1$	$L1\Longrightarrow 1$	$L1\Longrightarrow 1$	$L1\Longrightarrow 1$	$L1\Longrightarrow 1$	$H2\Longrightarrow 2$
		$H2\Longrightarrow 1$									
3	$H2\Longrightarrow 1$	$H3\Longrightarrow 1$	$H2\Longrightarrow 1$	$H2\Longrightarrow 1$	$H2\Longrightarrow 1$	$H2\Longrightarrow 1$	$H2\Longrightarrow 1$	$H2\Longrightarrow 1$	$H2\Longrightarrow 1$	$H2\Longrightarrow 1$	$L2\Longrightarrow 2$
4	$H3\Longrightarrow 1$	$L2\Longrightarrow 1$	$H3\Longrightarrow 1$	$L2\Longrightarrow 1$	$H3\Longrightarrow 1$	$H3\Longrightarrow 1$	$H3\Longrightarrow 1$	$H3\Longrightarrow 1$	$H3\Longrightarrow 1$	$H3\Longrightarrow 1$	$H3\Longrightarrow 3$
5	$H4\Longrightarrow 1$	$H1\Longrightarrow 2$	$L2\Longrightarrow 1$	$L3\Longrightarrow 1$	$L2\Longrightarrow 1$	$L2\Longrightarrow 1$	$L2\Longrightarrow 1$	$L2\Longrightarrow 1$	$L1\Longrightarrow 2$		$L3\Longrightarrow 3$
6	$L2\Longrightarrow 1$	$L1\Longrightarrow 2$	$H2\Longrightarrow 2$		$H4\Longrightarrow 1$	$H4\Longrightarrow 1$	$L3\Longrightarrow 1$	$L1\Longrightarrow 2$	$H2\Longrightarrow 2$		$H4\Longrightarrow 4$
7	$H1\Longrightarrow 2$	$H2\Longrightarrow 2$	$H3\Longrightarrow 2$			$H1\Longrightarrow 2$	$L1\Longrightarrow 2$	$H2\Longrightarrow 2$	$H1\Longrightarrow 3$		$L4\Longrightarrow 4$
8	$L1\Longrightarrow 2$	$H3\Longrightarrow 2$	$L1\Longrightarrow 2$			$H2\Longrightarrow 2$	$H2\Longrightarrow 2$		$L2\Longrightarrow 1$		$H5\Longrightarrow 5$
9	$H1\Longrightarrow 3$	$L2\Longrightarrow 2$	$H2\Longrightarrow 3$			$L1\Longrightarrow 2$	$H3\Longrightarrow 2$		$L1\Longrightarrow 3$		$L5\Longrightarrow 5$
10	$H2\Longrightarrow 2$	$L3\Longrightarrow 1$	$L1\Longrightarrow 3$				$L1\Longrightarrow 2$		$H2\Longrightarrow 3$		
11	$L1\Longrightarrow 3$		$H3\Longrightarrow 3$						$H3\Longrightarrow 3$		
12	$H3\Longrightarrow 2$		$L2\Longrightarrow 2$								
13	$L2\Longrightarrow 2$		$L3\Longrightarrow 1$								
14	$L3\Longrightarrow 1$										

TABLE IV. Intersubband transitions corresponding to row 2 under each panel in Figs. 4 and 5. Experimental data are from Refs. 16 and 18–21.

	Transitions for row 2 in Figs. 4 and 5										
No.	4(a)	4(b)	4(c)	4(d)	4(e)	4(f)	4(g)	5(a)	5(b)	5(c)	5(d)
1	$H1\Longrightarrow 1$	$H1\Longrightarrow 1$	$H1\Longrightarrow 1$	$H1\Longrightarrow 1$	$H1\Longrightarrow 1$	$H1\Longrightarrow 1$	$H1\Longrightarrow 1$	$H1\Longrightarrow 1$	$H1\Longrightarrow 1$	$H1\Longrightarrow 1$	$H1\Longrightarrow 1$
2	$L1\Longrightarrow 1$	$L1\Longrightarrow 1$	$L1\Longrightarrow 1$	$L1\Longrightarrow 1$	$L1\Longrightarrow 1$	$L1\Longrightarrow 1$	$L1\Longrightarrow 1$	$L1\Longrightarrow 1$	$L1\Longrightarrow 1$	$L1\Longrightarrow 1$	$L1\Longrightarrow 1$
3	$H2\Longrightarrow 1$	$H2\Longrightarrow 1$	$H2\Longrightarrow 1$	$H2\Longrightarrow 1$	$H2\Longrightarrow 1$	$H2\Longrightarrow 1$	$H2\Longrightarrow 1$	$H2\Longrightarrow 1$	$H2\Longrightarrow 1$		$H2\Longrightarrow 2$
4	$H3\Longrightarrow 1$	$H3\Longrightarrow 1$	$H3\Longrightarrow 1$	$H3\Longrightarrow 1$	$H3\Longrightarrow 1$	$H3\Longrightarrow 1$	$H3\Longrightarrow 1$	$H3\Longrightarrow 1$	$H3\Longrightarrow 1$		$L2\Longrightarrow 2$
5	$L2\Longrightarrow 1$	$L2\Longrightarrow 1$	$L2\Longrightarrow 1$	$L2\Longrightarrow 1$		$L2\Longrightarrow 1$	$H1\Longrightarrow 2$	$L2\Longrightarrow 1$	$H1\Longrightarrow 2$		$H3\Longrightarrow 3$
6	$H4\Longrightarrow 1$	$H1\Longrightarrow 2$	$H4\Longrightarrow 1$	$L3\Longrightarrow 1$		$H1\Longrightarrow 2$	$L1\Longrightarrow 2$	$H1\Longrightarrow 2$	$L1\Longrightarrow 2$		$L3\Longrightarrow 3$
7	$H1\Longrightarrow 2$	$L1\Longrightarrow 2$	$H1\Longrightarrow 2$			$L1\Longrightarrow 2$	$L2\Longrightarrow 1$		$H2\Longrightarrow 2$		$H4\Longrightarrow 4$
8	$L1\Longrightarrow 2$	$H2\Longrightarrow 2$	$L1\Longrightarrow 2$			$H2\Longrightarrow 2$	$L3\Longrightarrow 1$		$H3\Longrightarrow 2$		$L4\Longrightarrow 4$
9	$H2\Longrightarrow 2$	$H3\Longrightarrow 2$	$H2\Longrightarrow 2$						$L2\Longrightarrow 1$		$H5\Longrightarrow 5$
10	$H3\Longrightarrow 2$	$L2\Longrightarrow 2$	$H3\Longrightarrow 2$						$L3\Longrightarrow 1$		$L5\Longrightarrow 5$
11	$L2\Longrightarrow 2$		$L2\Longrightarrow 2$						$H1\Longrightarrow 3$		
12	$L3\Longrightarrow 1$		$H1\Longrightarrow 3$						$L2\Longrightarrow 2$		
13	$H1\Longrightarrow 3$		$L1\Longrightarrow 3$						$L1\Longrightarrow 3$		
14			$H2\Longrightarrow 3$						$H2\Longrightarrow 3$		
15			$H3\Longrightarrow 3$						$H3\Longrightarrow 3$		
16			$L2\Longrightarrow 3$						$L2\Longrightarrow 3$		
17									$L3\Longrightarrow 2$		

it seems impossible to judge from Figs. 4 and 5 which one of our three calculated spectra fits best to the measured data.

Experimental data on the energy differences $\hbar\omega_{CBn,HHm}-\hbar\omega_{CB1,HH1}$ and $\hbar\omega_{CBn,LHm}-\hbar\omega_{CB1,LH1}$ are available. The photoreflectance measurement[22] was performed at room temperature at four different positions of a MQW sample $GaAs/Al_{0.24}Ga_{0.76}As$ with $d_A=150$ Å and $d_B=220$ Å. In the photoluminescence experiment,[23] a $GaAs/Al_{0.3}Ga_{0.7}As$ MQW sample with $d_A=199$ Å and $d_B=191$ Å was measured at low temperature. These data are listed in Table VI, where the first column δE labels the intersubband transitions with the same notation as the one used in Tables III–V. The four columns $P1$, $P2$, $P3$, and $P4$ contain the data measured at four different positions of the MQW sample. Our calculated

TABLE V. Intersubband transitions corresponding to row X under each panel in Figs. 4 and 5. Experimental data are from Refs. 16 and 18–21.

	Transitions for row X in Figs. 4 and 5										
No.	4(a)	4(b)	4(c)	4(d)	4(e)	4(f)	4(g)	5(a)	5(b)	5(c)	5(d)
1	$H1\Longrightarrow 1$	$H1\Longrightarrow 1$	$H1\Longrightarrow 1$	$H1\Longrightarrow 1$	$H1\Longrightarrow 1$	$H1\Longrightarrow 1$	$H1\Longrightarrow 1$	$H1\Longrightarrow 1$	$H1\Longrightarrow 1$	$H1\Longrightarrow 1$	$H1\Longrightarrow 1$
2	$L1\Longrightarrow 1$	$L1\Longrightarrow 1$	$L1\Longrightarrow 1$	$L1\Longrightarrow 1$	$L1\Longrightarrow 1$	$L1\Longrightarrow 1$	$L1\Longrightarrow 1$	$L1\Longrightarrow 1$	$L1\Longrightarrow 1$	$L1\Longrightarrow 1$	$L1\Longrightarrow 1$
			$H2\Longrightarrow 1$						$H2\Longrightarrow 1$		$H2\Longrightarrow 2$
3	$H2\Longrightarrow 1$	$H2\Longrightarrow 1$	$H3\Longrightarrow 1$	$H2\Longrightarrow 1$	$H2\Longrightarrow 1$	$H2\Longrightarrow 1$	$H2\Longrightarrow 1$	$H2\Longrightarrow 1$	$H3\Longrightarrow 1$	$H2\Longrightarrow 1$	$L2\Longrightarrow 2$
4	$H3\Longrightarrow 1$	$H3\Longrightarrow 1$	$H1\Longrightarrow 2$	$H3\Longrightarrow 1$	$H3\Longrightarrow 1$	$H3\Longrightarrow 1$	$H3\Longrightarrow 1$	$L2\Longrightarrow 1$	$H1\Longrightarrow 2$		$H3\Longrightarrow 3$
5	$H1\Longrightarrow 2$	$L2\Longrightarrow 1$	$L2\Longrightarrow 1$			$L2\Longrightarrow 1$	$L2\Longrightarrow 1$		$L2\Longrightarrow 1$		$L3\Longrightarrow 3$
6	$L1\Longrightarrow 2$	$H1\Longrightarrow 2$	$H2\Longrightarrow 2$			$H1\Longrightarrow 2$	$H1\Longrightarrow 2$		$H2\Longrightarrow 2$		$H4\Longrightarrow 4$
			$L1\Longrightarrow 2$						$L1\Longrightarrow 2$		
7	$H2\Longrightarrow 2$	$L1\Longrightarrow 2$	$H3\Longrightarrow 2$			$L1\Longrightarrow 2$	$L1\Longrightarrow 2$		$H3\Longrightarrow 2$		$L4\Longrightarrow 4$
8	$H3\Longrightarrow 2$	$H2\Longrightarrow 2$	$L2\Longrightarrow 2$			$H2\Longrightarrow 2$	$H2\Longrightarrow 2$		$L2\Longrightarrow 2$		$H5\Longrightarrow 5$
9	$L2\Longrightarrow 1$	$H3\Longrightarrow 2$	$H1\Longrightarrow 3$						$L3\Longrightarrow 1$		$L5\Longrightarrow 5$
10	$H4\Longrightarrow 2$	$L2\Longrightarrow 2$	$H2\Longrightarrow 3$						$H1\Longrightarrow 3$		
			$L1\Longrightarrow 3$								
11	$H1\Longrightarrow 3$		$L3\Longrightarrow 1$						$H2\Longrightarrow 3$		
									$L1\Longrightarrow 3$		
12	$L1\Longrightarrow 3$		$L2\Longrightarrow 3$						$H3\Longrightarrow 3$		
13	$H2\Longrightarrow 3$		$L3\Longrightarrow 2$						$L3\Longrightarrow 2$		
14	$H3\Longrightarrow 3$								$L2\Longrightarrow 3$		
15	$L2\Longrightarrow 2$								$L3\Longrightarrow 3$		
16									$L2\Longrightarrow 2$		
17									$L3\Longrightarrow 3$		

TABLE VI. A comparison between the calculated intersubband transition energies and the measured ones (Refs. 22 and 23). See the text for details.

	Photoreflectance data (meV)				Calculation (meV)	
δE	$P1$	$P2$	$P3$	$P4$	No. 1	No. 2
$H2 \Longrightarrow 2$	29±3	30±3	31±3	30±3	30.52	32.46
$H3 \Longrightarrow 3$	80±4	84±4	86±4	89±4	80.67	85.66
$h4 \Longrightarrow 4$	146±4	148±4	152±4	154±4	148.67	157.50
$h5 \Longrightarrow 5$	215±6	219±6	228±6	232±5	229.71	241.52
$L2 \Longrightarrow 2$	44±10	45±10	44±10	44±10	40.59	44.64
$L3 \Longrightarrow 3$	107±10	110±10	114±10	109±10	100.05	108.77
$L4 \Longrightarrow 4$	188±10	196±10	224±10	227±10	172.06	196.32
	Photoluminescence data (meV)					
$H2 \Longrightarrow 2$	31.6±1.5				36.53	36.73
$H1 \Longrightarrow 3$	91.7±1.0				98.61	97.58

energies under column no. 1 are derived from using the first set of parameter values with $Q=0.89$, and those under column no. 2, are computed with the second set of parameter values and $Q=0.85$. Again in this table the fit of the no. 1 transition energies to the photoluminescence and the photoreflectance data is equally good as the fit of the no. 1 calculated transition energies.

V. REMARKS

Since our computation is numerically exact, any question on the so-obtained results is directly related to the adequacy of the model and the accuracy of the parameter values used in the calculation. We have shown that the weak dependence of the subband structure on the value of β is an intrinsic property of the simple model. While our numerical study on this one-dimensional model is already very extensive, the excitonic state and the intersubband transition intensity need to be fully investigated. In our opinion, without such knowledge it is almost impossible to determine the correct value of the conduction-band offset coefficient Q. Of course, the experimental accuracy on the measurement of x also affects the agreement between calculated and the observed spectra.

ACKNOWLEDGMENTS

This work was financially supported by the Swedish Natural Science Research Council under Grant No. NFR-FFU-3996-302.

*Permanent address: Institute of Physics, University of Trondheim–NTH, N-7034 Trondheim, Norway.

[1]T. Gora and F. Williams, Phys. Rev. **177**, 1179 (1969).
[2]O. von Roos, Phys. Rev. B **27**, 7547 (1983).
[3]Q.-G. Zhu and H. Kroemer, Phys. Rev. B **27**, 3519 (1983).
[4]R. A. Morrow and K. R. Brownstein, Phys. Rev. B **30**, 678 (1984).
[5]R. A. Morrow, Phys. Rev. B **35**, 8074 (1987).
[6]S. R. White and L. J. Sham, Phys. Rev. Lett. **47**, 879 (1981).
[7]K. B. Kahen and J. P. Leburton, Phys. Rev. B **33**, 5465 (1986).
[8]T. Ando and S. Mori, Surf. Sci. **113**, 124 (1982).
[9]I. Galbraith and G. Duggan, Phys. Rev. B **38**, 10057 (1988).
[10]G. T. Einevoll and P. C. Hemmer, J. Phys. C **21**, L1193 (1988).
[11]J. Thomsen, G. T. Einevoll, and P. C. Hemmer, Phys. Rev. B **39**, 12 783 (1989).
[12]S. Adachi, J. Appl. Phys. **58**, R1 (1985).
[13]T. F. Kuech, D. J. Wolford, R. Potemski, J. A. Bradley, K. H. Kelleher, D. Yan, J. P. Farrell, P. M. S. Lesser, and F. H. Pollak, Appl. Phys. Lett. **51**, 505 (1987).
[14]P. Lawaetz, Phys. Rev. B **4**, 3460 (1971).
[15]S. C. Shen (private communication).
[16]C. Weisbuch, R. C. Miller, R. Dingle, A. C. Gossard, and W. Wiegmann, Solid State Commun. **37**, 219 (1981).
[17]R. Dingle, W. Wiegmann, and C. H. Henry, Phys. Rev. Lett. **33**, 827 (1974).
[18]W. T. Masselink, P.J. Pearah, J. Klem, C. K. Peng, H. Morkoç, G. D. Sanders, and Y.-C. Chang, Phys. Rev. B **32**, 8027 (1985).
[19]R. C. Miller, D. A. Kleinman, W. A. Nordland, Jr., and A. C. Gossard, Phys. Rev. B **22**, 863 (1980).
[20]B. V. Shanabrook, O. J. Glembocki, and W. T. Beard, Phys. Rev. B **35**, 2540 (1987).
[21]O. J. Glembocki, B. V. Shanabrook, N. Bottka, W. T. Beard, and J. Comas, Appl. Phys. Lett. **46**, 970 (1985).
[22]P. Parayanthal, H. Shen, F. H. Pollak, O. J. Glembocki, B. V. Shanabrook, and W. T. Beard, Appl. Phys. Lett. **48**, 1261 (1986).
[23]R. C. Miller, D. A. Kleinman, O. Munteanu, and W. T. Tsang, Appl. Phys. Lett. **39**, 1 (1981).